


# AQUARELLUS: A NUMERICAL TOOL TO CALCULATE ACCUMULATION OF PARTICULATE MATTER IN DRINKING WATER DISTRIBUTION SYSTEMS

Joost van Summeren<sup>1</sup>, Amitosh Dash<sup>2</sup>, Mark Morley<sup>3</sup>, Luuk de Waal<sup>4</sup>, Jip van Steen<sup>5</sup>

<sup>1,2,3,4,5</sup>KWR Water Research Institute, Groningenhaven 7, 3433 PE, Nieuwegein (The Netherlands)

<sup>5</sup>Currently at: Het Waterschapshuis, Stationsplein 89, 3818 LE, Amersfoort (The Netherlands)

<sup>1</sup>  [Joost.van.Summeren@kwrwater.nl](mailto:Joost.van.Summeren@kwrwater.nl), <sup>2</sup> [Amitosh.Dash@kwrwater.nl](mailto:Amitosh.Dash@kwrwater.nl), <sup>3</sup> [Mark.Morley@kwrwater.nl](mailto:Mark.Morley@kwrwater.nl),

<sup>4</sup> [Luuk.de.Waal@kwrwater.nl](mailto:Luuk.de.Waal@kwrwater.nl), <sup>5</sup> [Jip.van.Steen@kwrwater.nl](mailto:Jip.van.Steen@kwrwater.nl).

## Abstract

Despite preventive measures, turbid (vernacular: “discolored”) distributed drinking water is still a common cause for customer complaints across the world. Discoloration events are caused by the accumulation of particulate matter in drinking water distribution systems (DWDSs) and subsequent remobilization during hydraulic events, although uncertainties remain concerning the specific accumulation and transport processes. For Dutch DWDSs, it is plausible that microscopic particles originating at treatment plants contribute substantially to the particulate matter that resides in DWDSs, and that physical processes *within* the distribution network are cardinal in the subsequent transport during distribution.

*Aquarellus* is a predictive numerical tool that has been developed to predict the location and amount of accumulated particulate material in DWDSs. It integrates hydraulic calculations using the EPANET toolbox with a particle transport module that is based on a description of gravitational settling, particle stagnation, bed load transport, and resuspension of particles in distribution pipes, depending on the shear stress near the pipe wall. Despite the particle transport calculations being very computationally intensive, parallelization allows for simulating distribution network sizes that are common to Dutch water utilities (100s of km total pipe length). The user can assign the injection of multiple particle species corresponding to temporal patterns at multiple source locations. A graphical user interface handles user IO and the visualization of geographical maps as well as time-dependent build-up of particulate material across the distribution network and within individual pipes.

To characterize particle properties (critical input parameters) encountered in DWDSs, we performed lab experiments on nine samples from one Flemish (chlorinated drinking water) and two Dutch (non-chlorinated) DWDSs to determine particle size distributions, mass density, mobility thresholds, and a measure for gravitational settling. Using the outcomes of these lab experiments, a sensitivity test with a range of input parameters was performed in *Aquarellus*. This helped determine how the variation in the relevant input parameters influences the calculated spatial patterns of accumulated particulate matter – a measure for the discoloration risk. We compared the modeling results to turbidity measurements from systematic cleaning actions in a real-life Dutch distribution network. Finally, we discuss the potential for applying the tool to assist the planning of cleaning actions and monitoring programs.

## Keywords

Discoloration, water quality modelling, drinking water distribution system.

## 1 INTRODUCTION

Despite preventive measures, turbid (vernacular: “discolored”) distributed drinking water is still a common cause for customer complaints across the world. Discoloration events are caused by the accumulation of particulate matter in drinking water distribution systems (DWDSs) and subsequent remobilization during hydraulic events [1], although uncertainties remain concerning the specific accumulation and transport processes. For Dutch DWDSs, it is suspected that microscopic particles originating from treatment plants contribute substantially to the particulate matter that resides in DWDSs, and that physical processes *within* the distribution network are cardinal in the subsequent transport during distribution.

Observational evidence suggest that the accumulation of particulate material in DWDSs often occurs in a repeatable spatial and temporal patterns and diminishes above a threshold hydraulic vigor (e.g. [2, 3]). This formed the basis for design and application of self-cleaning networks in The Netherlands that have been applied in The Netherlands since the 1990 and that have been shown to reduce the number of customer complaints [4]. These observations also suggests that can be described with a predictive model .

Several models for discoloration in DWDSs have been developed previously. Richardt et al. (2009) [5] developed a model to optimize flushing intervals to prevent deposit growth in pipes. These predictions are based on maximum daily velocities from a hydraulic simulation and deposit measurements for all pipes in the study area. The Particle Sediment Model [6] includes the processes of particle settling, resuspension, and wall deposition. However, the potentially important process of bed-load transport is absent from this model. The semi-empirical Variable Condition Discoloration Model (VCDM) [7] builds on the Prediction and Control of Discolouration in Distribution Systems (PODDS), [8]. VCDM provides a mathematical formulation for the simultaneous removal (by means of erosion) and build-up (by means of adhesion to pipe walls) of particulate material, depending on the material strength in relation to the actual shear stress. VCDM has been validated for UK transport mains. However, theoretical considerations [9] suggest that conditions and mechanisms may differ from DWDSs with different source qualities due to other treatment processes or non-chlorinated Dutch systems that include self-cleaning network layouts. It is emphasized that the location and amount of particle accumulation in DWDSs cannot be reliably predicted on the basis of actual hydraulic conditions of single pipe segments, or even its hydraulic history. This is because the evolution of sediments relies on the accumulation *history* that includes bed-load transport and recurrent resuspension-settling that can result in complex transport of material through the distribution network.

This paper presents the development of *Aquarellus*, a numerical tool to predict the accumulation of particulate material in DWDSs. It integrates hydraulic calculations using the EPANET toolbox with a particle transport module (PTM) that is based on a description of gravitational settling, particle stagnation, bed load transport, and resuspension of particles in distribution pipes, depending on the shear stress near the pipe wall [10]. To characterize particle properties (critical input parameters for *Aquarellus*) encountered in Dutch DWDSs, we performed lab experiments on nine field samples collected by three water utilities to determine particle size distributions, mass density, on which the particle settling velocity depends. Based on the outcomes of these lab experiments, a sensitivity analysis with a range of input parameters was performed to determine the influence on calculated spatial patterns of accumulated particulate matter– a measure for the discoloration risk. The potential for applying *Aquarellus* in assisting in the planning of cleaning actions and network monitoring is discussed.

## 2 METHOD

### 2.1 Conceptual framework and model assumptions

The theoretical framework of *Aquarellus* was formulated in a previous study that investigated the leading processes governing particle transport and discoloration events in DWDSs [10]. This study assessed which particle transport mechanisms are dominant for hydraulic conditions and particle properties that are typical of Dutch distribution pipelines in DWDSs. The theoretical framework identifies three modes of particle mobility that are discriminated based on the shear stress exerted by the turbulent flow near the pipe wall,  $\tau_b$  (Figure 1). The shear stress exerted is closely related to the flow velocity of the water ( $u_f$ ). The dimensionless Shields number ( $\theta$ ) expresses the ratio between the driving (shear stress) and resisting forces to particle mobility, in which the driving and resisting forces depend on the particle properties:

$$\theta = \frac{\tau_b}{(\rho_p - \rho_f)gd_p} \quad (1)$$

$$\tau_b = \frac{\rho_f u_f^2 C_f}{8} \quad (2)$$

with  $\rho_p$  and  $\rho_f$  the mass densities of the particulate material and drinking water, respectively,  $g$  the gravitational acceleration,  $d_p$  the particle diameter, and  $C_f$  the Darcy friction factor. Eq. (1) and (2) can be combined as:

$$\theta = \frac{u_f^2 C_f}{8sgd_p} \quad (3)$$

where  $s$  is the excess mass density of particles relative to that of water:  $s \equiv \frac{(\rho_p - \rho_f)}{\rho_f}$  and  $g$  the gravitational acceleration. For the settling velocity,  $u_s$ , we used Stokes' Law which assumes free settling of spherical and incompressible particles in a fluid:

$$u_s = \frac{gsd_p^2}{18\nu_f} \quad (4)$$

With  $\nu_f$  kinematic viscosity of the fluid. Constant values were assumed for  $\rho_f$  ( $1 \cdot 10^3 \text{ kg m}^{-3}$ ),  $\nu_f = 1 \cdot 10^{-6} \text{ m}^2 \text{ s}^{-1}$ , and  $C_f = 0.02$ .

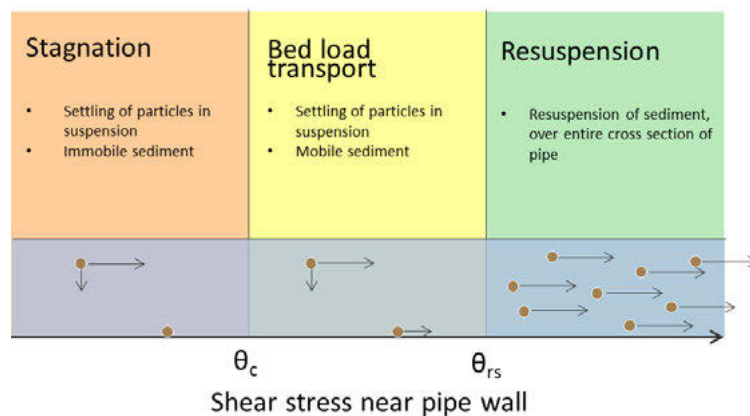


Figure 1. Conceptual representation of the particle transport model (modified from [10]).

The modes of particle mobility illustrated in *Figure 1* are:

i. *Particle settling under the influence of gravity followed by stagnation*

At low velocities, when the Shields number  $\theta$  is below the threshold value for incipient motion ( $\theta < \theta_c$ , red area in *Figure 1*), particles in suspension settle according to Stokes' Law to the invert of the pipe under the influence of gravity and, once settled, remain immobile.

ii. *Particle settling under the influence of gravity followed by bed-load transport*

At shear stress conditions between the critical Shields number for incipient motion,  $\theta_c$ , and for particle entrainment by resuspension,  $\theta_{rs}$  (i.e.  $\theta_c < \theta < \theta_{rs}$  yellow area in *Figure 1*), particles in suspension settle, but particles at the pipe's invert move by means of bed-load transport. *Aquarellus* assumes the bed-load velocity to increase linearly from 0 to  $uu_f$  when  $\theta$  increases from  $\theta_c$  to  $\theta_{rs}$ .

iii. *Particle resuspension by hydraulic forces*

At shear stresses above the critical Shields number for resuspension ( $\theta > \theta_{rs}$ , green area in *Figure 1*), it is assumed that all particles resuspend instantly. The particles are redistributed uniformly over the cross section of the pipe and move with velocity  $u_f$ .

The above-mentioned processes were identified as the dominant physical processes for particle diameters and flow conditions common to distribution pipes with fully developed pipe flow in Dutch DWDSs. Other mechanisms related to turbulent motion-particle interaction are likely relevant, although probably not dominant, including turbulent diffusion, turbulent dispersion, turbophoresis, gradual rather than abrupt transitioning to bed-load transport and resuspension (see [10] for a more extensive discussion). Irregular pipe structure (due to e.g. culverts, bends, and appurtenances) may further complicate the local hydraulic conditions and the associated particle transport. Furthermore, complex interactions with microbiological (e.g. biofilm formation) and/or chemical processes (e.g. coagulation) may also influence the mobility and accumulation of particulate material but are difficult to describe and were kept out of the scope of the current study.

## 2.2 Architecture of *Aquarellus*

The overall architecture of *Aquarellus* is depicted in *Figure 2*. A graphical user interface (GUI) is coupled to a computational core that combines:

- (i) the functionality of EPANET [11] to calculate hydraulic transport in the DWDSs and
- (ii) the particle transport module (PTM) calculates the transport of particulate matter across distribution pipes, according to the theoretical framework discussed in Section 2.1.

The bed load transport velocity of particles can have any velocity between zero and the fluid velocity, depending on the actual Shields number. This requires a fine spatial resolution of particle transport in the streamwise direction. Consequently, the PTM computations are generally more expensive than the hydraulic computations.

From the concentration of particulate material at the source nodes, *Aquarellus* calculates the corresponding number of particles that enter the DWDS. To keep a practically feasible memory load, the particles are combined into packages that move collectively. This particle collation number is user-defined and 1 million by default. Particle packages are injected and subsequently transported through the DWDS at two user-specified time steps that can be set independently between 1 and 60 s. The accuracy of the results of *Aquarellus* were verified using a series of benchmarks of small (9-node) network models for a model time of 30 days. The particle masses

were accurate within  $\sim 1\%$  and  $\sim 6\%$ , respectively for injection and transport time steps of 1 and 60 seconds, respectively.

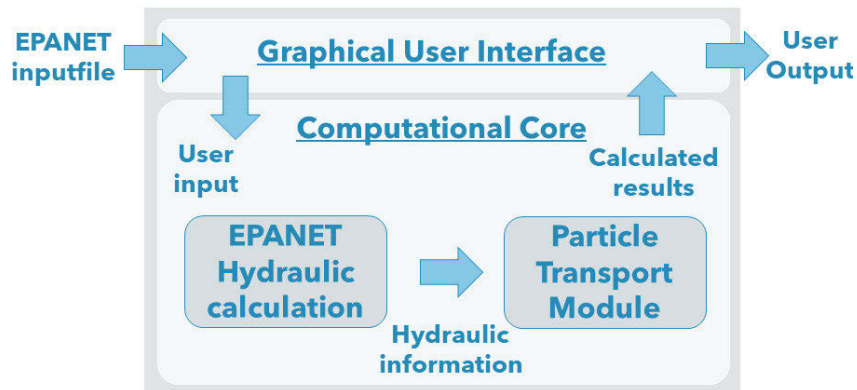


Figure 2. Architecture of the numerical tool.

The memory use and calculation time of *Aquarellus* primarily depend on the total network length, the amount of particle packages in the network model, and the numerical resolution settings. Multi-threading and code optimization were performed to enable calculation of full-scale hydraulic network models on a commonly used laptop quadcore (Intel Core i7, 16 GB). Specifically, a memory of 16 GB was sufficient to calculate a typical hydraulic network model with a total pipe length 500 km in 48 hours.

In practical terms, calculations with *Aquarellus* are performed by providing a modified EPANET input file in which the user defines multiple network junctions as source nodes. For each source node, the incoming mass concentration of particulate material is provided either as a constant baseline level or time-dependent pattern. It is also possible to assign sources of distinct particle material properties at a single node, thereby creating a “multi-species” source, and interpret the distinct species separately. Within the GUI, the user can assign the material properties of each material species, and settings for the numerical resolution and graphical representation of the simulation results that includes exportable tables, graphs, and maps of accumulated masses in the DWDS. The maps make use of geographical information from OpenStreetMap [12]. An impression of the GUI of *Aquarellus* is shown in Figure 3.

### 3 DETERMINING MATERIAL PROPERTIES OF PARTICULATE MATERIAL

#### 3.1 Motivation

The material properties of particles affect the particle transport and the resulting spatial configuration of stagnant and bed-load particulate material that forms in the DWDS (hereinafter referred to as “sedimentation configuration”). In the calculations of *Aquarellus*, the relevant material properties are: the particle mass density ( $\rho_p$ ), particle diameter ( $d_p$ ), and the critical shear stresses at which particles mobilize as bed-load transport ( $\theta_c$ ) and resuspend ( $\theta_{rs}$ ). Within the framework of *Aquarellus* an increase in particle size ( $d_p$ ) and density ( $\rho_p$ ) result in: (i) a faster particle settling velocity,  $u_s$  (through Stokes’ Law) and (ii) a lower dimensionless shear stress (Shields number  $\theta$ ) which, in turn, results in a lower propensity to particle mobility, i.e. a larger hydraulic disturbance is required for the transition from stagnation to bed-load transport and from bed-load transport to resuspension.

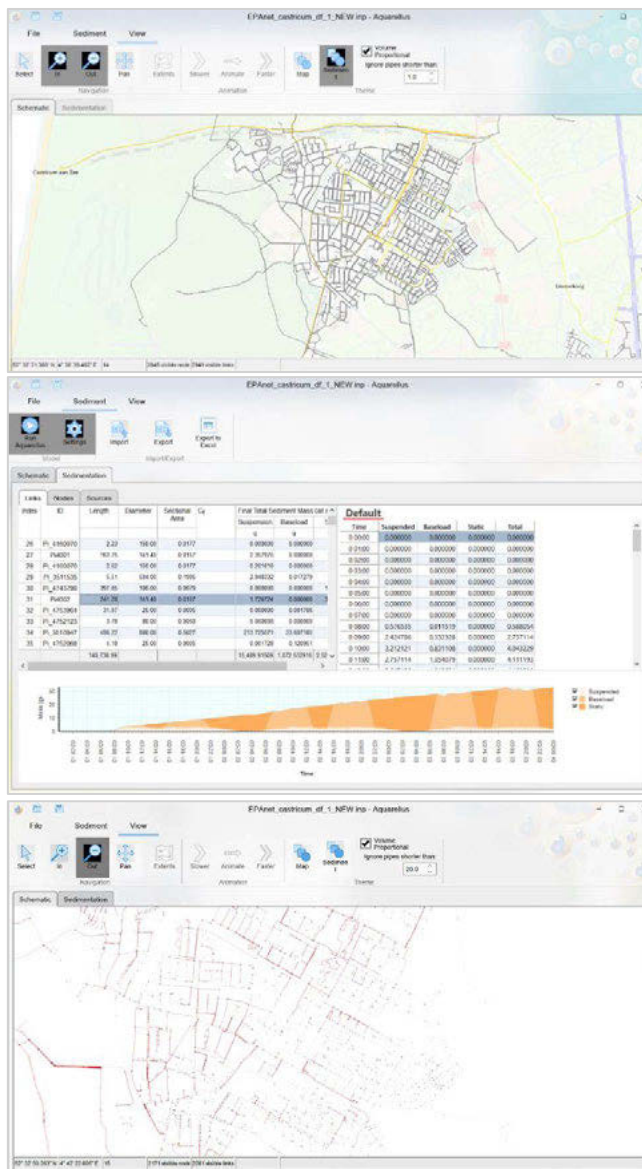


Figure 3. Impression of *Aquarellus*' Graphical User Interface showing examples of (top) map of imported hydraulic network model projected on top of geographical map, (middle) modelling result showing masses of suspended, bed-load, and stagnant particle masses for each pipe (left table), time series of particle masses (right table and graph at the bottom), and (bottom) map of sediment masses per pipe.

Previous measurements have given some information on  $d_p$  and  $\rho_p$  and lab experiments provide insight into the mobility thresholds  $\theta_c$  and  $\theta_{rs}$  [10]. To determine the range of input parameters that can be expected in Dutch and Flemish DWDSs, a series of nine field samples were collected and analyzed in a series of lab experiments. The nine samples are taken in 3 distribution areas at three different locations, aimed at gaining insight into the variation between and within distribution areas. The results form the basis of the sensitivity analysis described in Section -.

### 3.2 Sampling of drinking water using disruptive actions

Three water companies conducted disturbance tests in the summer of 2020 at three locations in Sint Jans klooster (Vitens), Spijkenisse (Evides), and Neerpelt (De Watergroep). The disturbance test were performed following a protocol similar to that of flushing actions. Samples of 20 L were

collected from hydrants installed at PVC distribution pipes (80 to 110 mm). The areas were selected for a suspected high risk of particulate accumulation. Thus, turbidity values are not indicative of the drinking water quality that these water utilities distribute. To avoid misportrayal, the areas have been anonymized as Areas *A*, *B*, and *C*. In each area, three sample locations were selected: 'near', 'mid', and 'far' from the supply location and within a pipeline length of 2 to 5 km. The samples locations were positioned on the same flow path, meaning that the same water flow passed through the three locations 'near', 'mid', and 'far' for each area. Locations 'near' and 'far' were separated by a minimum pipe length of 2 to 5 km, depending on the area .

### 3.3 Laboratory tests to characterize particles in samples of drinking water

#### Particle settling test

Particle settlement tests were performed for all nine samples using a beaker setup. From each sample, a homogenized subsample of 2 L was taken at 7 cm above the bottom of the beaker glass.

The beaker glass was filled to a height of 14 cm and was subsequently mixed with a stirrer for 10 minutes at 150 r.p.m. after which turbidity was measured for 24 h using a Hach 2100 IQ turbidity meter. The rate of turbidity decrease was quantified by calculating the half-life time ( $\tau_{1/2}$ ) (from an exponential fit of the measured values). A short  $\tau_{1/2}$  is taken as an indicator value for a high settling velocity,  $u_s$ . It must be noted that this is a global measure of a mixture of particles types with different individual settling velocities.

#### Particle size determination

The particle size distribution was determined for the 9 samples using a PAMAS particle counter in particle size intervals of 1-3  $\mu\text{m}$ ; 3-5  $\mu\text{m}$ ; 5-10  $\mu\text{m}$ ; 10-20  $\mu\text{m}$ ; 20-35  $\mu\text{m}$ ; 35-60  $\mu\text{m}$ ; and 60-100  $\mu\text{m}$ . The size was interpreted as particle diameter ( $d_p$ ). It was verified that the particle numbers of samples were within the interval for accurate measurements by diluting the original samples (5 times and 10 times dilution) and verifying the corresponding dilution factors in the results.

#### Particle density estimation

All nine samples were analyzed in the lab to estimate the particle density,  $\rho_p$ , following these steps:

- Determine the volume of the wet sediment,  $V_{wet}$ . In this context, "wet sediment" refers to the turbid part of the sample after 72 h of settling in a measuring cone beaker.
- Determine the dry weight,  $m_{dry}$ , after heating at 105 °C of the 0.45  $\mu\text{m}$  filtrated residue of 1 L of homogenized sample.
- The particle density,  $\rho_p$ , was estimated as the density of the "wet" sediment:

$$\rho_p = \frac{1}{V_{wet}} \left( \rho_w [V_{wet} - \frac{m_{dry}}{\rho_{dry}}] + m_{dry} \right) \quad (4)$$

The term between []-brackets expresses the volume of the *water* fraction in the wet sediment. The parameter  $\rho_{dry}$  is not readily measured and remains undetermined in this study. This introduces an uncertainty in  $\rho_p$ , which converges from its minimum value,  $\rho_{dry} = \rho_w$  at  $\rho_{dry} = 0$ , to its maximum value at  $\rho_{dry} = \infty$ . It can be shown that the convergence (in terms of the relative excess density) depends on  $\rho_{dry}$  as:  $s(\rho = \rho_{dry}) / s(\rho = \infty) = 1 - \rho_w / \rho_{dry}$ . In the remainder of this paper we assume a negligible dry sediment volume by assuming an infinite  $\rho_{dry}$ .

### 3.4 Results of laboratory experiments

The main results of the laboratory experiments are shown in Table 1. The main findings are:

- The turbidity measured at the beginning of the settling experiment (when the sample is fully mixed) is hereinafter referred to as the “initial turbidity”. It shows a strong variation both *across* and *within* the three distribution areas, ranging from 60 to 150 NTU (Area A), 0 NTU (Area B), and 0 to 40 NTU (Area C). The initial turbidity and the dry weight increase with an increasing number of particles in the sample, as expected.
- A fraction of 40% to 70% of the particles are in the 1 – 3  $\mu\text{m}$  range (relative to particle count in the 1- 100  $\mu\text{m}$  range). The number of particles decreases approximately logarithmically with particle size and with mildly varying fractions at location 1, 2, and 3 (not shown).
- The half-life time  $\tau_{1/2}$  shows a wider variation between the three areas (averages of 5.5, 11.7, and 6.0 h for Area A, B, and C, respectively) than within each area (ranges of 4.1 to 6.8 h, 9.4 to 13.3 h, and 4.4 to 9.2 h, respectively). Although  $\tau_{1/2}$  cannot be readily translated to the settling velocity, it is useful to try to put these in perspective. A 10  $\mu\text{m}$  particle of  $\rho_p = 1100 \text{ kg}\cdot\text{m}^{-3}$  has a settling velocity of  $5.45\cdot 10^{-5} \text{ m}\cdot\text{s}^{-1}$  and would sink across the height of the water column in the beaker (14 cm) during 7.1 h which of the same order as the measured values.

Table 1. Lab experiment results of properties of particles in drinking water sampled during disturbance tests. (\*): Could not be estimated accurately because of the small dry weight.

Sample location	Settling test		Particle count		Lab analysis	
	Initial turbidity (NTU)	Half-life time turbidity, $\tau_{1/2}$ (h)	Log <sub>10</sub> (N) (number of particles)	Fraction of 1-3 $\mu\text{m}$ particles (% of total)	Dry weight ( $\text{mg}\cdot\text{L}^{-1}$ )	Estimated particle density ( $\text{kg}\cdot\text{m}^{-3}$ )
A <sub>near</sub>	149	4.1	6.33	68.7	100	1052.6
A <sub>mid</sub>	82.3	5.5	6.19	59.4	64	1045.7
A <sub>far</sub>	56.1	6.8	5.91	64.1	42	1084.0
B <sub>near</sub>	3.32	12.4	4.62	68.7	3.2	*
B <sub>mid</sub>	3.35	9.4	4.25	59.4	4.6	*
B <sub>far</sub>	1.85	13.3	4.11	64.1	2.1	*
C <sub>near</sub>	3.94	9.2	4.58	66.5	5.7	*
C <sub>mid</sub>	42.3	4.5	5.54	47.0	63	1018.0
C <sub>far</sub>	20.8	4.4	4.95	40.0	37	1018.5

- For each of the three areas (but not for the nine samples combined), particle settling is faster (shorter  $\tau_{1/2}$ ) for more turbid samples. A correlation based on chance cannot be ruled out. Another possible explanation is that fast-settling particles concentrate more readily at locations than slow-sinking particles, which at the same flow rate would settle over a larger area.



- For Area A, a lower initial turbidity and longer  $\tau_{1/2}$  are measured at locations further away from the pumping station (locations ‘near’, ‘mid’, and ‘far’, respectively). This would be in line with preferential settling close to the source location, especially for fast-settling particles. However, Area B and C do not show this relation, suggesting that other mechanisms are important.
- For five samples, sufficient material was present to derive densities of the wet sediment, calculated according to Eq. 4 and assuming an infinite  $\rho_{dry}$ . The estimated particle densities range from 1018 to 1084 kg/m<sup>3</sup>.

## 4 SENSITIVITY OF CALCULATED SEDIMENTATION CONFIGURATIONS TO PARTICLE PROPERTIES

### 4.1 Scenarios of the Castricum distribution network

Next, we investigated how the sedimentation configurations calculated with *Aquarellus* are influenced by variations in the particle diameter ( $d_p$ ), particle density ( $\rho_p$ ), and the shear stress mobility thresholds for critical motion ( $\theta_c$ ) and resuspension ( $\theta_{rs}$ ). To this end, a series of scenarios was run of which a selection of seven will be discussed in this study. The input parameters used in the reference (RFS) and sensitivity scenarios (S1 to S6) are shown in Table 2. In the present study, it is assumed that the ratio between these two Shields numbers is constant at 1:10.

The range of values for  $d_p$  and  $\rho_p$  are based on the lab test results presented in Chapter 3. The reference model values of  $d_p$  and  $\rho_p$  are slightly larger than the average measured values; this was done to focus on results with sufficient accumulation in the DWDS models of 30 days (i.e. relatively fast settling velocities). The critical Shields numbers for incipient particle motion and resuspension are based on empirical relationships for rectangular channels documented in the sediment transport literature (see [10] for details and references).

Table 2. Input parameters of *Aquarellus* for seven model scenarios used in the sensitivity analysis. RFS refers to the reference scenario. S1 to S6 refer to scenarios in which parameters indicated in boldface differ from the RFS.

Quantity	Symbol	RFS	S1	S2	S3	S4	S5	S6
Particle mass density (kg · m <sup>-3</sup> )	$\rho_p$	1100	<b>1050</b>	<b>1150</b>	1100	1100	1100	1100
Dimensionless mass density (-)	S	0.1	<b>0.05</b>	<b>0.15</b>	0.1	0.1	0.1	0.1
Particle diameter (µm)	$d_p$	10	10	10	<b>8.8</b>	<b>11.2</b>	10	10
Settling velocity (Stokes) (µm·s <sup>-1</sup> )	$u_s$	54.5	<b>22.3</b>	<b>82.0</b>	<b>42.2</b>	<b>68.3</b>	54.5	54.5
Critical Shields number for incipient motion (-)	$\theta_c$	1	1	1	1	1	<b>0.5</b>	<b>2</b>
Critical Shields number for resuspension (-)	$\theta_{rs}$	10	10	10	10	10	<b>5</b>	<b>20</b>

The sensitivity analysis was applied to the 141 km hydraulic network model of Castricum, a municipality of ca. 35,000 inhabitants in the province of North-Holland, The Netherlands. Its

network is part of the distribution area of PWN water utility and has a relatively simple supply structure (single water supply; no water tanks; no substantial water exchange with connecting areas).

The hydraulic network model is shown in Figure 4 (pipe diameters and velocity during the morning demand peak in frame (a) and (b), respectively). The supply is located in the Southwest of the area and feeds the Castricum municipality via two transport mains as indicated. In the Northern half of the area, the main flow is in the clockwise direction around Castricum municipality and supplies this area at several locations. All scenarios were calculated for a model period of 30 days. Initially the network contains no sediment, and the particles are introduced at the source at a concentration of 0.023 mg/L. A demand pattern for a standard weekday was deliberately repeated throughout the model period, which makes the results easier to interpret.

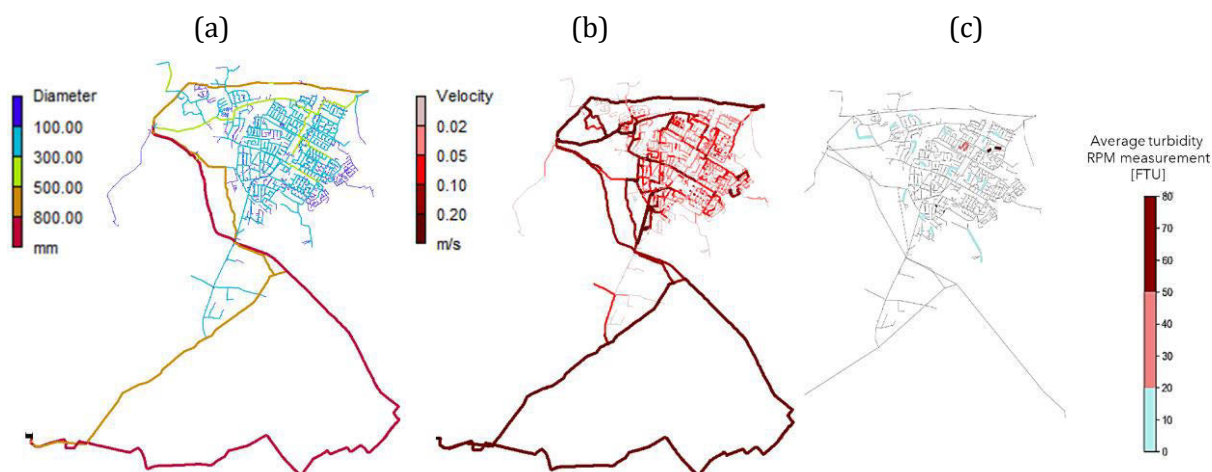


Figure 4. DWDS of Castricum (PWN) with (a) pipe diameter, (b) flow velocity at 8AM, and (c) RPM field measurements of turbidity. No measurements were available for the pipes indicated in grey in frame (c).

Figure 4c shows an overview of 22 turbidity measurements from the period 2018-2020. The measurements were performed by PWN following the Resuspension Potential Method (RPM) [13], a measuring protocol aimed at measuring the presence and mobility of particulate material in pipe segments with diameters in the range of 50-200 mm. The RPM consists of a controlled and reproducible increase of 0.35 m/s in addition to the actual velocity at the time of measuring. This hydraulic disturbance was created by opening a hydrant on an isolated pipe segment to create a unidirectional flushing. PWN maintained the disturbance for a duration of 15 minutes and the turbidity was monitored every 3 minutes of which the average was used in this study. All the RPM measurements used in this study had a preceding RPM measurements three years earlier, thus creating similar RPM disturbance histories. The area did not experience major disruptions (from flushing actions, major construction works, or network extensions) in the evaluation period, although minor disruptions did occur (such as minor construction works and operational actions). These are beneficial properties when comparing calculated sediment masses to field measurements.

#### 4.2 Sedimentation configurations of model scenarios

The sedimentation configurations after 30 days of simulation at 12 AM (midnight) for the reference scenario (see Table 2) is shown in Figure 5. It shows that distribution pipes with and without substantial sediment masses can be in close proximity; and most distribution pipes with high accumulation levels are relatively close to where the distribution area branches off from the transport mains.

(a)

(b)



Figure 5. (a) Calculated sedimentation configuration for the reference scenario (RFS) of Castricum after 30 days, and (b) zoom-in of the same scenario. The encircled red areas show distribution pipe clusters of anomalously large sediment masses. The black dotted circles and ellipses show area where >300 mm transport mains connect to distribution pipes smaller than 300 mm.

The sensitivity of sedimentation configurations to input parameters is demonstrated with a selection of results in Figure 6 (cf. to the reference scenario in Figure 5). The sensitivity analysis captures the progressive increase of  $d_p$  (from 0.88 to 1 to 1.12  $\mu\text{m}$ ),  $\rho_p$  (from 1050 to 1100 to 1150  $\text{kg}\cdot\text{m}^{-3}$ ) and the mobility thresholds for incipient motion and resuspension (from  $\theta_c = 0.5$ ;  $\theta_{rs} = 5$  to  $\theta_c = 1$ ;  $\theta_{rs} = 10$  to  $\theta_c = 2$ ;  $\theta_{rs} = 20$ ).

For each of the three tests, an increase in the parameter resulted primarily in (i) a larger amount of sediment is present in the DWDS after 30 days and, (ii) a larger fraction of sediments closer to where the transport mains supply Castricum municipality (i.e. the dotted circles and ellipses in Figure 5b). These two phenomena are stronger for the variation of  $\rho_p$ , than for  $\theta_c$  and  $\theta_{rs}$ , than for  $d_p$  over the parameter ranges tested.

These results reflect that bigger and heavier particles are associated with a faster settling velocity (linear dependence  $u_s \propto s \cdot d_p^2$ ) and a lower propensity to particle mobilization (linear dependence  $\theta \propto s \cdot d_p$ ), while a simultaneous increase in  $\theta_c$  and  $\theta_{rs}$  results in a lower propensity to particle mobilization. Although these outcomes may seem obvious from *Aquarellus*' theoretical framework, it is emphasized here that the calculated sediment mass cannot be reliably predicted on the basis of actual hydraulic conditions of single pipe segments, or even its hydraulic history. This is because the evolution of sediments relies on the sedimentation history that includes bed-load transport and recurrent resuspension-settling that can result in complex transport of material through the distribution network.

Based on a visual interpretation of Figure 5 and Figure 6, two neighborhoods in the Castricum DWDS stand out in expected to have above-average sediment masses (the transport mains that feed the municipality are not taken into account in this analysis). These sediment 'hotspots' are indicated in Figure 5b with the red ellipses. Although their spatial extent varies, these locations are also present as hotspots in most of the scenarios of the sensitivity test analysis. The results also show that within these hotspot locations, the sediment masses are spatially irregular, i.e. clean pipes can coexist adjacent to contaminated pipes, even in hotspot locations. A more quantitative analysis is required to substantiate this visual interpretation.

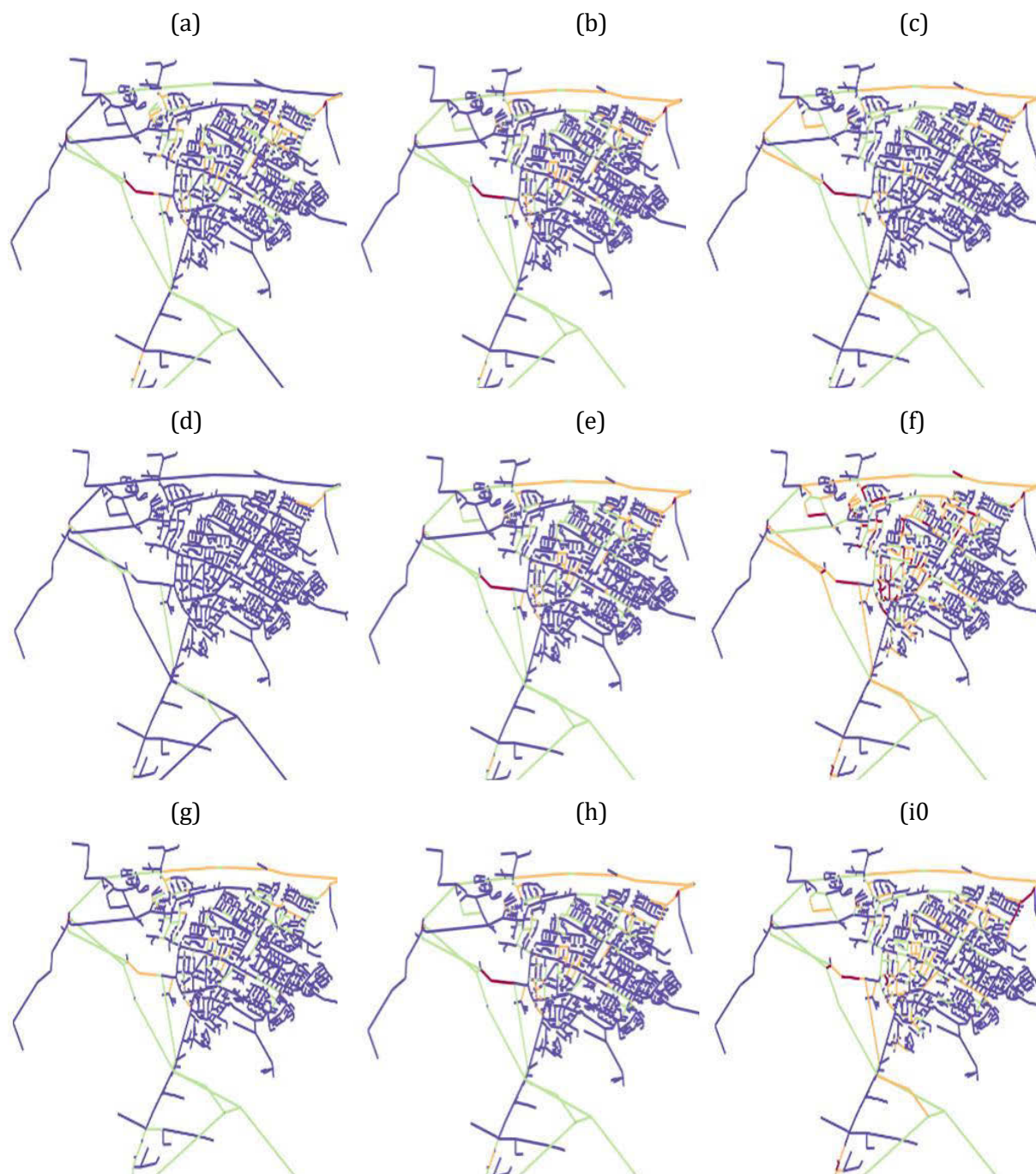


Figure 6. Calculated sediment configurations after 30 days at 12 AM for Castricum DWDS. The reference model is shown in frame (b), (e), and (h) and was assigned input parameters  $\rho_p = 1100 \text{ kg}\cdot\text{m}^{-3}$ ,  $d_p = 1\cdot 10^{-6} \text{ m}$ ,  $\theta_c = 1$  and;  $\theta_{rs} = 10$ . Input parameters that deviate from the reference model are (a) model S1 ( $\rho_p = 1050 \text{ kg}\cdot\text{m}^{-3}$ ), (b) S2 ( $\rho_p = 1150 \text{ kg}\cdot\text{m}^{-3}$ ), (c) S3 ( $d_p = 0.88\cdot 10^{-6} \text{ m}$ ), (d) S4 ( $d_p = 1.12\cdot 10^{-6} \text{ m}$ ), (e) S5 ( $\theta_c = 0.5$ ;  $\theta_{rs} = 5$ ), and (f) S6 ( $\theta_c = 2$ ;  $\theta_{rs} = 20$ ). Color legend is identical to Figure 5.

### 4.3 Comparing results to turbidity measurements

A proper validation of the modelling results based on the RPM measurements in Castricum was difficult to make for a number of reasons.

#### *Hydraulic uncertainty*

Although it was a deliberate choice to perform the numerical calculations with recurring 24 h demand patterns, this also simplified the hydraulic variations that are expected in a real-life DWDS. Those variation originate from daily and seasonal total demand variations, the stochastic nature of customer demand, and the occurrence of small network interventions. Despite the area having been relatively “quiet” in terms of large network operations and cleaning actions (see Section 4.1), smaller interventions are known to have occurred throughout the evaluation period.

In general, this level of detail of the hydraulic variations is not available for DWDSs. Nevertheless improved knowledge on the uncertainty imposed on the results can be obtained, e.g. by extending the sensitivity analysis with stochastic demand modelling and hydraulic variations related to daily and seasonal demand variations and network interventions.

#### *Limited monitoring resolution of turbidity measurements*

Despite the fact that the area being monitored in a systematic way over more than a decade, an even finer resolution of measurements would be required to make a convincing comparison between the contaminations calculated with *Aquarellus* and those inferred from RPM measurements.

This level of detail would require an even more extensive measuring program. While this is feasible for specific areas, large-scale implementation would involve big investments and take many years. To address this issue, a comparison at a larger spatial scale could be facilitated by aggregating both the results of *Aquarellus* and the available measurements on the scale of neighborhoods.

#### *Sediment mass vs. RPM turbidity*

The RPM is devised to monitor the *mobile fraction* of particulate material, rather than *all* material in a pipe segment. However, in the sensitivity tests the presence of *all* sediment mass was analysed. A more precise comparison is possible, but this require the simulation of multi-species sediments that would respond selectively to RPM shear stresses.

It is known that sediment mass relates to turbidity in an approximately linear fashion for a particular distribution area, but that the slope of this dependence can vary strongly between areas. This makes it difficult to interpret the absolute levels of sediment masses predicted by *Aquarellus*. Consequently, the predicted sedimentation configurations are best compared to field measurements in a relative sense (e.g. by dividing the sediment masses by the average sediment mass in the study area).

With the above issues in mind, it is not possible to draw strong conclusions from the comparative analysis. Of the two identified hotspots in the results, the Northeastern hotspot coincides with the two locations where the highest turbidity values were measured (cf. Figure 5, Figure 4c, and Figure 5b). The Southwestern hotspot coincides with few measurements, and no high-turbidity measurements in its vicinity.

## 5 CONCLUDING REMARKS

This paper presents the numerical tool *Aquarellus* that was developed to predict the accumulation of particulate material from source locations in a DWDS via particle settling, bed-load transport and resuspension. The code allows for calculations of hydraulic network models of several hundreds of km on a standard laptop computer. The user can specify the properties of particulate material (diameter  $d_p$ , mass density  $\rho_p$ , and shear stress thresholds to incipient motion  $\theta_c$  and resuspension  $\theta_{rs}$ ). This material can enter the network from multiple (user-specified) source locations according to temporal concentration patterns.

The lab experiments presented in this paper demonstrate the variation of particle properties ( $d_p$ , estimated  $\rho_p$ , and half-life time  $\tau_{1/2}$  of the turbidity in a settling experiment, which was used as a proxy for the setting velocity  $u_s$ ) found across and within three Dutch and Flemish DWDSs. The results of a sensitivity analysis show the influence of  $d_p$ ,  $\rho_p$ ,  $\theta_c$  and  $\theta_{rs}$  on the absolute levels of sedimentation configurations in the model of the real-life DWDS of Castricum. The results from *Aquarellus* suggest the presence of two hotspot areas with a higher propensity to particle accumulation than their surroundings.

Although an attempt was made to validate the predictions of *Aquarellus* with field measurements of a full-scale DWDS, it was difficult to derive strong conclusions from this comparative study. The reason lies mainly in (i) a limited knowledge of hydraulic conditions at the level of individual pipes, related to stochastic customer demand, daily and seasonal demand variations, as well as operational anomalies, and (ii) a limited monitoring resolution of turbidity measurements; although thoroughly monitored (pilot) areas exist, this limitation will remain innate to most DWDSs for the foreseeable future. A more thorough validation with field data is required to gain confidence in the predictive power of *Aquarellus* (and, by extension, a deterministic approach).

Several future modelling steps can address some of these limitations. A more extensive sensitivity analysis could investigate the influence of plausible demand fluctuation (stochastic, seasonal, etc.) on sedimentation configurations. In light of the (limited) available turbidity measurements, the aggregation of calculated sediment masses and measured turbidity values (e.g. at scale of neighborhoods), would allow for a more significant comparison between predictions and observations (albeit on a lower spatial resolution). From the measurement perspective, it is recommended to monitor turbidity over long periods in a standardized manner to gain further insight in contamination pattern of areas that can be used for validation purposes.

The potential benefit for system operations of *Aquarellus* lies in the prioritization of subregions of faster than average accumulation of particulate material through prioritization. As such, *Aquarellus* can help the planning of cleaning actions and measuring programs. Ultimately, with enough confidence in its predictive power, *Aquarellus* could also be used to further optimize the self-cleaning capacity of DWDSs [1, 2, 14]. Although more thorough validation is desired, *Aquarellus* may already be used as a prioritization aid to plan cleaning actions or measuring campaigns.

## 6 ACKNOWLEDGEMENTS

The research presented in this paper was conducted within a project of the Joint Research Program (BTO) of the Dutch Water Companies and De Watergroep. We greatly appreciated the help of Evi Loozen (De Watergroep), Henk de Kater (Evides), and Jan Pot (Vitens) in organising the field sampling campaigns and Matthijs Rietveld (PWN) in making available the Castricum hydraulic model and measurements.

## 7 REFERENCES

- [1] J. Vreeburg, “Discolouration in drinking water systems: a particular approach”, Ph.D. Thesis, Delft University of Technology, 2007.
- [2] E. Blokker, J. Vreeburg, P. Schaap, and J. van Dijk, “The self-cleaning velocity in practice”. 12th Annual Conference on Water Distribution Systems Analysis (WDSA). 2011.
- [3] S. Mounce, E. Blokker, S. Husband, W. Furnass, P. Schaap, and J. Boxall. “Multivariate data mining for estimating the rate of discolouration material accumulation in drinking water distribution systems. IWA J. Hydroinformatics, 18, pp.96-114, 2016.
- [4] E. Blokker, P. Schaap, and Vreeburg, “Self-cleaning networks put to the test”. IWA Leading Edge conference on Strategic Asset Management (LESAM 2007), Lisbon, 2009.
- [5] S. Richardt, A. Korth, and B. Wricke, ”Model for the calculation of optimized flushing concepts”, TECHNEAU: Safe Drinking Water from Source to Tap, Ed. By T. van den Hove, and C. Kazner., IWA Publishing, London, 2009.
- [6] G. Ryan, P. Mathes, G. Haylock, A. Jayaratne, J. Wu, N. Noui-Mehidi, C. Grainger, and B. Nguyen, “Particles in Water Distribution Systems.” Rpt. No. 33. The Cooperative Research Centre for Water Quality and Treatment, 2008.
- [7] W. Furnass, R. Collins, S. Husband, R. Sharpe, S. Mounce, and J. Boxall, “Modelling both the continual and erosion and regeneration of discolouration material in drinking water distribution systems”. Water Sci. Technol. 14, pp. 81-90, 2014.
- [8] J. Boxall, A. Saul, J. Gunstead, and N. Dewis, "A novel approach to modelling sediment movement in distribution mains based on particle characteristics". Water Software Systems, Ch. 1: Theory and Applications, Eds.: B. Ulnacki B. Coulbeck, J. Rance. Hertfordshire, UK, 2001.
- [9] P. van Thienen, J. Vreeburg, and E. Blokker, “Radial transport processes as a precursor to particle deposition in drinking water distribution systems". Water Res., 45, pp. 1807-1817, 2011.
- [10] J. van Summeren & M. Blokker, “Modeling particle transport and discoloration risk in drinking water distribution networks”, Drink, Water Eng. Sci. 10, 2017, pp.99-107, 2017.
- [11] L. Rossman, “EPANET 2 Users Manual”, U.S. Environmental Protection Agency, Washington, D.C., EPA/600/R-00/057, 2000.
- [12] OpenStreetMap. <https://www.openstreetmap.org/> (2022).
- [13] J. Vreeburg, P. Schaap, and J. van Dijk, “Measuring discoloration risk: resuspension potential method,”in M. van Loosdrecht & J. Clement (Eds.), 2nd IWA Leading-Edge Conference on Water and Wastewater Treatment Technologies, Prague, Czech Republic. 2005, pp. 123-132.
- [14] E. Abraham, E. Blokker, I. Stoianov, “Decreasing the discolouration risk of drinking water distribution systems through optimized topological changes and optimal flow velocity control”. J. Wat. Res. Planning and Management. 144 (2), 2018.